EXPERIMENTAL INVESTIGATION OF FLUID-STRUCTURE INTERACTION IN THE CASE OF HYDROGEN/AIR DETONATION IMPACTING A THIN PLATE

Alexis Dancelme[1,2], Sergey Kudriakov[1], Etienne Studer[1], and Christian Tenaud[2]

(1) - Université Paris-Saclay, CEA, Service de Thermo-hydraulique et de Mécanique des Fluides, 91191, Gif-sur-Yvette, France.

(2) - Université Paris-Saclay, CNRS, CentraleSupélec, Laboratoire EM2C, 91190, Gif-sur-Yvette, France.

ABSTRACT

In recent years, the use and development of hydrogen as a carbon-free energy carrier have grown. However as hydrogen is flammable with air, safety issues are raised. In the case of ignition, especially in confined space, the flame can accelerate and reach the detonation regime, causing severe structural damage [1].

To assess these safety issues, it is required to understand the fluid-structure interaction in the case of a detonation impacting a deformable structure and to quantify and model this interaction [2]. At the CEA (Commissariat à l'énergie atomique et aux energies alternatives) a combustion tube experimental facility [3] for studying the fluid-structure interaction in the case of hydrogen combustion has been developed. Several Photomultipliers and Pressure sensors are placed along the tube to monitor the flame acceleration and the detonation location. A fluid-structure interaction (FSI) module or a non-deformable flange can be placed at the end of the tube. Post-processing of the sensor's signal will provide insight into the occurring phenomena inside the tube.

Several experimental campaigns have been conducted, with various initial conditions and configurations at the end of the tube. In this contribution, the experiments resulting in a detonation are presented. First, the recorded pressure and velocities will be compared to theoretical values coming from combustion models [4] [5]. Secondly, the impulse before and after reflection for thin plate and non-deformable flange will be compared to quantify the energy transmitted to the plate and the influence of the fluid-structure interaction on the reflected shock.

NOMENCLATURE

Abbreviations

FSI: Fluid-Structure Interaction

BR: Blockage ratio

PX: Pressure sensor X (with X the sensor number)

PMX: Photomultiplier X (with X the sensor number)

Symbols

ρ: density ($kg.m^{-3}$)

p: pressure (bar)

U_{CJ}: Chapman-Jouguet velocity (m/s)

γ: Heat capacity ratio

T: Temperature (K)

R: Radius of the plate (m)

t: Thickness of the plate (m)

I: Impulse (Pa.s)

σ_0: Static yield stress (MPa)

ϕ_c: Damage number

δ: Centrale deflection (m)

1.0 INTRODUCTION

Hydrogen safety is a major challenge in the development of hydrogen as an energy carrier as well as in nuclear power-plant accidental scenario. When hydrogen is released, especially in a confined space, the ignition of a flammable atmosphere can cause the flame to accelerate and reach the detonation regime, causing several structural damages to the surrounding structures. There is several examples of major structural damages caused by the explosion of a flammable hydrogen-air atmosphere, in the nuclear industry (Three Mile Island (1979), Fukushima Daiichi (2011)) or for Hydrogen storage facility (Oslo, Norway (2019) and Gangneung, South Korea (2019)). To continue the development of future hydrogen related technology these safety issue must be assessed.

In order to assess these safety issues, the physical phenomena of the flame acceleration and the structural deformation as well as their interaction must be understood. To investigate these phenomena the SSEXHY facility is available, a combustion tube with a fluid-structure interaction module. This facility enable us to measure the flame acceleration and position as well as the deformation of simple structure such as thin plate or thin cylinder.

In the following work, a series of experiments will be presented. The experiments presented here have been conducted with a thin plate as deformable structure and hydrogen/air mixture close to stoichiometry to promote the mixture to reach the detonation regime. The analysis of these experimental data and the comparison to theoretical models will be presented in this article.

2.0 THEORY

In this work, the two main phenomena studied are the propagation of a detonation in tubes and the deformation of thin plate under an impulsive load. These two phenomena are well documented theoretically, experimentally and numerically.

2.1 Chapman-Jouguet detonation

In certain cases and favorable conditions, a burning mixture can accelerate to reach high propagation velocities. In extreme cases, transition from deflagration to detonation can occur giving a combustion wave propagating at supersonic speed. In such wave, we shall distinguish the induction zone, where the shock will raise the pressure and the temperature facilitating the ignition of the reactants, and then the reaction zone where the combustion reaction occurs. However, these two zones being very small they can be approximate to an only discontinuity to facilitate their study. The propagation of detonation has been well studied theoretically, the first classical theory of detonation comes from Chapman [6] and Jouguet [7] that derived a simple theory for detonation in parallel. In the so-called Chapman-Jouguet theory, the detonation is seen as a one-dimensional reactive wave traveling at the Chapman-Jouguet detonation speed. It is possible to compute the Chapman-Jouguet state using a Newton-Raphson algorithm iterating on the conservation equations. Values of the thermodynamic quantities for the Chapman-Jouguet state for a stoichiometric hydrogen/air mixture are shown in Table 1. Reference values has been computed with the Chemical Equilibrium with Application code [8] from NASA, and the calculated values from a Newton-Raphson algorithm implemented in our team.

Table 1: Chapman-Jouguet state for stoichiometric hydrogen/air mixture

Quantities	Reference	Calculated values
Pressure (bar)	15.80	15.78
Temperature (K)	2943	2941
Density ($kg.m^{-3}$)	1.55	1.54

Chapman-Jouguet velocity ($m.s^{-1}$)	1965	1968
Products velocity ($m.s^{-1}$)	1089	1091
Products heat capacity ratio	1.16	1.16

2.2 Plate deformation under an impulsive load

In a second place when the detonation is impacting the plate, this impact will cause the plate to deform under the load of the detonation. Pressure evolution of a detonation is characterized by a sudden pressure spike at the detonation arrival followed by a decay to the equilibrium state imposed by the boundary condition at the ignition end. This type of load can be described as an impulsive load. Nurick et al. [9] [10] [11] have extensively studied the deformation of thin plate under such impulsive load. These articles are reviewing several studies with various origin for the impulsive load, such as explosive sheet attached to the thin plate or explosive with standoff distance under water. For purpose of comparison it is possible to use the characteristic quantities in order derive non-dimensionnal quantities. A so-called damage number can be derived and is noted ϕ_c, for circular plate is written as follow:

$$\phi_c = \frac{I}{\pi t^2 \sqrt{\rho \sigma_0}} = \frac{I_p R}{t^2 \sqrt{\rho \sigma_0}}, \quad (1)$$

Where R is the radius of the plate in mm, t the thickness of the plate in mm, ρ the material density in $kg.m^{-3}$ and σ_0 the static yield stress in Pa and $I_p = \frac{I}{\pi R^2}$. In this case, the impulse I is expressed in $kg.m.s^{-1}$ and the pressure impulse expressed in Pa.s. Then this damage number has been correlated to the ratio between the central deflection δ and the plate thickness using the available experimental data:

$$\frac{\delta}{t} = 0.427\phi_c + 0.298, \quad (2)$$

Here we are dealing with gaseous detonation, we expect that there could be differences in the plate behavior. Nevertheless, it would be interesting to compare with the solid explosive deformation formula. The main parameter in equations (1) and (2) is the impulse, which is relatively easy to compute for the experiments presented in this contribution.

3.0 DESCRIPTIONS OF THE EXPERIMENTS

In this section, a general description of the SSEXHY experimental facility and its measurement system will be provided. The SSEXHY facility has been developed at the CEA to study the mechanisms of flame acceleration and fluid-structure interaction in the case of hydrogen/air flame [12]. The facility is composed of several sections that provide a great versatility to produce various experimental set-ups. Two main parts can be identified, the first part being a combustion tube to characterize the flame evolution. The second part, at the end of the tube, is a fluid-structure interaction (FSI) module with thin plate or a non-deformable flange.

In the second part of this section, the detonation experiments will be detailed with the corresponding set-up. Experiments with similar conditions (initial pressure, temperature and hydrogen concentration) where conducted with deformable plate and non-deformable flange. These two types of experiments can be compared to investigate the fluid-structure interaction.

3.1 Description of the SSEXHY Facility

The SSEXHY facility is composed of three sections of 1310 mm each and a straight adapter of 500mm, the total length is then 4430 mm. The inner diameter of each section is 120 mm. At one end lies the ignition system sealed with a blank flange, and at the other end several configuration either with or without FSI module are possible. In Fig. 1 a picture of the SSEXHY facility as well as a scheme of the

facility with its FSI module and safety dome. The combustion tube part is filled with annular obstacles of 5 mm thickness uniformly distributed along the tube, separated with 120 mm between each obstacle. These obstacles will enhance turbulence at the wall and thus promote flame acceleration. The blockage ratio of the annular obstacles is of 0.3, the blockage ratio is defined in Equation (3) where d is the unobstructed diameter and D is the tube internal diameter in mm. The details of the configuration used in this study are summarized in Table 1.

$$BR = 1 - \left(\frac{d}{D}\right)^2, \tag{3}$$

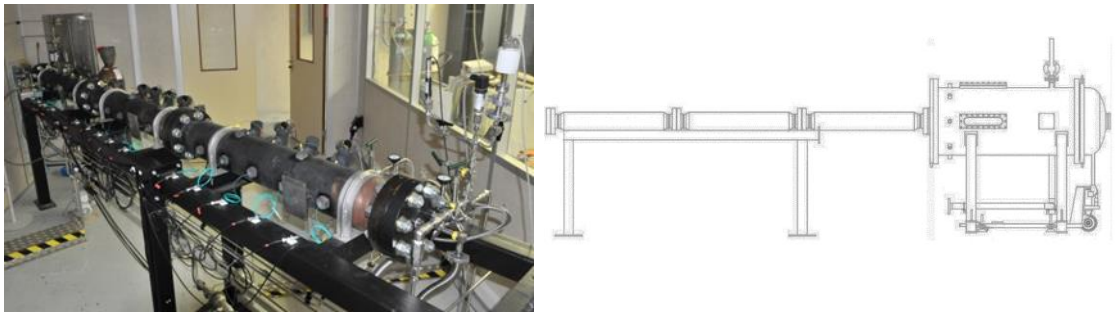

Figure 1: Left: Picture of the SSEXHY facility without FSI module
Right: Scheme of the SSEXHY facility with FSI module and safety dome mounted

Table 1: Used configuration of the SSEXHY facility

Length of the tube (mm)	Number of sections	End of the tube module
4430	Three sections + straight extension	Non-deformable flange, pressure sensors
4430	Three sections + straight extension	Thin plate

Along the combustion tube, several sensors are installed to monitor the physical phenomena occurring inside the combustion tube. The measurement system is composed of 14 photomultipliers (PM) and 6 pressure sensors (P) along the combustion tube. Then for the configurations with the straight extension, two pressure sensors are placed in the extension. The pressure sensors are Kistler piezo- electric sensors and three types of are used: 601A, 6001 and 7001. The 601A and 6001 are flush mounted and the 7001 are recess mounted. The other used sensors are Hamamatsu R11568 photomultiplier tubes. These sensors are regularly spaced along the combustion tube. For the Flange experiments a pressure sensor is placed at the center of the non-deformable flange. In Fig. 2 a scheme of the position of the PM and pressure sensors are shown and the positions of the sensors is summed up in Table 2.

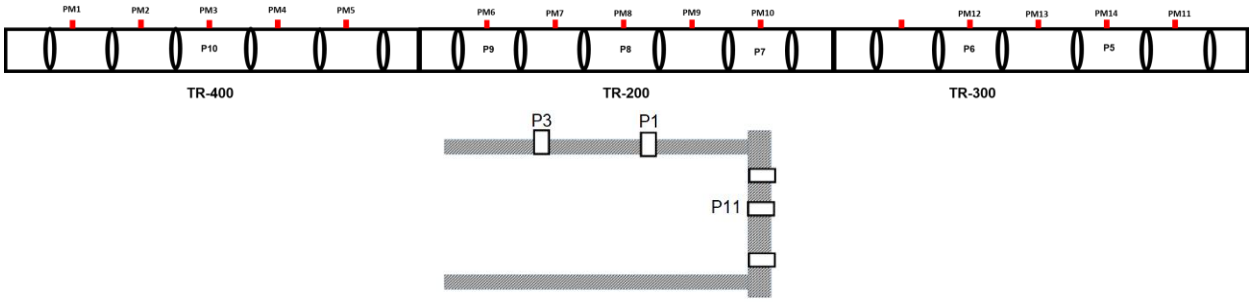

Figure 2: Schematic of the SSEXHY facility with sensors positioning

Table 2: Position of the sensors on the combustion tube of the SSEXHY facility

Position (mm)	Sensors
265	PM1
460	PM2
655	PM3-P10
850	PM4
1045	PM5
1575	PM6-P9
1770	PM7
1965	PM8-P8
2160	PM9
2355	PM10-P7
3080	PM12-P6
3275	PM13
3470	PM14-P5
4096	P3
4263	P1
4430	Non deformable flange or plate

3.2 Details of the Experiments

In this work, a mixture of Hydrogen and air is used. The brutto reaction for Hydrogen-air mixture combustion is shown in Equation (4). From this reaction, the stoichiometric ratio in mol% can be determined at $X_{H_2} = 29.5\%$.

$$H_2 + \frac{1}{2}(O_2 + 3.76N_2) \Leftrightarrow H_2O + 1.88N_2, \quad (4)$$

All experiments presented here have been realized in similar condition at atmospheric initial pressure and ambient initial temperature. The initial state inside the tube is a premixed mixture of hydrogen-air with a mole fraction $X_{H_2} \approx 29\%$, thus close to stoichiometry. To control the concentration of the mixture, a sample of the mixture is collected at each end of the tube to measure the concentration of Hydrogen via gas chromatography. The details of each experiments presented in this work are summed up in Table 3.

Table 3: List of the experiments presented in this work

Experiment name	Hydrogen mole fraction (%)	Plate thickness (mm)
Flange 1	28.9	x
Flange 2	29.2	x
Plate 1	29.0	1.01
Plate 2	29.4	0.48
Plate 3	29.1	0.48

For this series of experiments, plates are made of 304L stainless steel, a material frequently used the industry. The plate are then sealed with KLINGERSIL C-4430 gaskets. Besides the purpose of sealing the combustion tube, the gaskets have the purpose of limiting the mechanical constraints on the plate

due to the clamping. Material and geometrical properties of the plate and the gasket [13] are summed up in Table 4.

Table 4: Material and geometrical properties of the plate and gasket

	Plate	Gasket
Young's modulus (GPa)	199	1.8
Density ($kg.m^{-3}$)	7850	1750
Poisson's ratio (-)	0.275	-
Thickness (mm)	0.5 or 1	1.5
Exposed diameter (mm)	120	-
External diameter (mm)	175	-
Static yield stress (MPa)	210	-

4.0 EXPERIMENTAL RESULTS

In this section, the analysis of the experimental results and the quantification of the fluid structure interaction will be presented. First, a brief presentation of the methods used for the post-processing of the experimental data. Secondly, the monitoring of the detonation evolution along the tube and its comparison to the Chapman-Jouguet theory. Finally, the comparison of the impulses close to the tube end for Plate and Flange to quantify the FSI effects. In Fig. 3 can be observed the deformed shape of a 0.5mm plate after being impacted by a detonation.

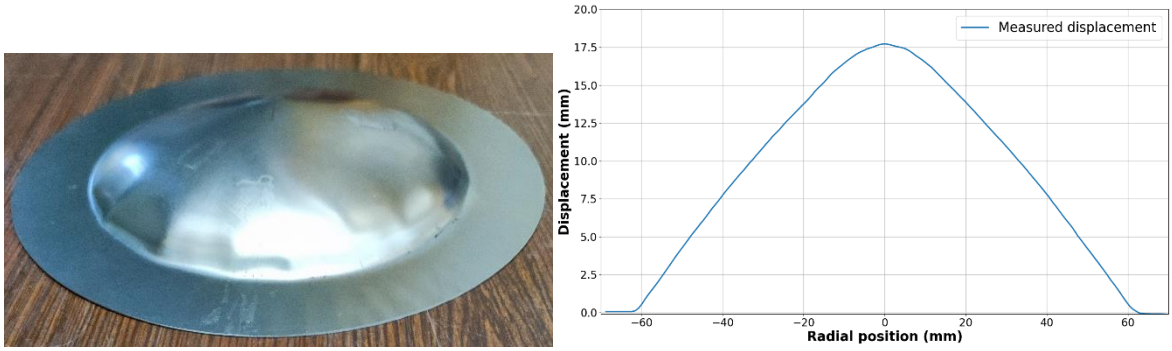

Figure 3: Post-experiment shape (left) and displacement measurement (right)

4.1 Methods used for the post-processing

From the available sensors along the combustion tube, the time of arrival of the shock (pressure sensor) and of the flame (photomultipliers) can be estimated. In the case of a detonation, those two times of arrival should be close. Then knowing the distance between two sensors the mean velocity between two sensors can be calculated for the PM and pressure sensors. From the pressure sensors along the tube and those on the non-deformable flange it is possible to estimate the impulse. The impulse characterize the load endured by the plate and is defined [14] in Equation 5.

$$I_p(t) = \int_{t_0}^{t_0+t} (p(t) - p_0)dt, \quad (5)$$

where t_0 (s) correspond to the time of arrival of the detonation, $p(t)$ and p_0 the signal of the pressure sensor and the reference pressure respectively in bar. For the post-processing all pressure signal are baselined to remove the remaining offset from the noise and residual pressure. Thus for the incoming detonation the value of p_0 is chosen as zero. However, as it can be observed in Fig. 4, for the second pressure pike corresponding to the reflected shock that the pressure is not back down to zero. Thus the

value of p_0 is defined as the pressure value at the time of arrival of the reflected shock. In some cases the noise on the pressure signal can be very harmful and limit the post-processing of the signal. In this case applying a low-pass filter to the signal to facilitate the analysis. In this work, a low-pass filter with a cutoff frequency of 60 kHz has been chosen. A comparison between the raw and filtered signal for the pressure sensor P1 is shown in Fig. 4.

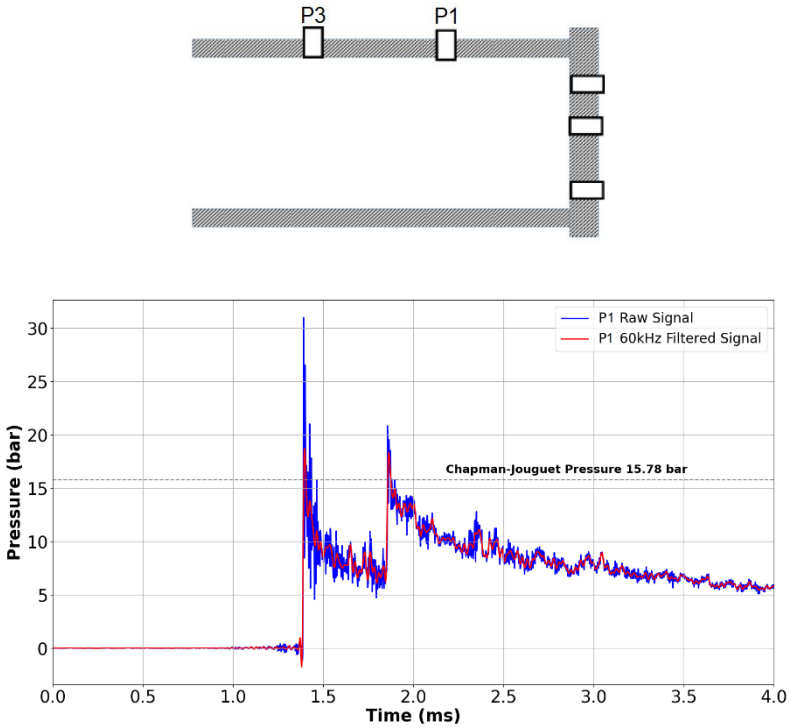

Figure 4: Raw versus filtered signal for P1 [Plate 1]

4.2 Detonation time of arrival and velocity

In order to assess that the flame has reached a detonation state two values can be extracted from the experimental data: the pressure spike and the velocity that can be compared to the Chapman-Jouguet pressure and velocity respectively. To compute the velocity the time of arrival at each pressure sensors and photomultipliers can be estimated looking at the strong variation caused by the detonation. For the pressure sensor the time of arrival is determined when the signal reach 5% of its maximum value. In previous work [12] an error estimation for these types of sensor has been performed, and the error margin is of 10 μs for the pressure sensors and of 5μs for the photomultipliers, that is a total of 15 μs of error margin. In Table 5, the differences of arrival time between the pressure sensors and photomultipliers are displayed. Some time differences are greater than the margin of error, these can be explained by the 3D structure of the detonation and the obstacles inside the combustion tube.

Table 5: Time of arrival difference for Plate 3 experiment

Position (mm)	Sensor pair	Plate 3 Δt (μs)
655	PM3-P10	15
1575	PM6-P9	8
1965	PM8-P8	5
2355	PM10-P7	8
3080	PM12-P6	18
3470	PM14-P5	3

Then from the time of arrival, a mean velocity between the sensors can be calculated. As well as for the time of arrival, the values of the velocities given by the type of sensors should be close to each other, and also close to the Chapman-Jouguet velocity in the case of a detonation. The comparison of the calculated velocities for the Plate 3 experiment can be observed in Fig. 5. Despite being close to the theoretical value, it can be observed that the calculated velocity are slightly lower compared to the Chapman-Jouguet velocity. This has been observed in previous work [15] and is due to the obstacles inside the combustion tube reducing the velocity of the detonation.

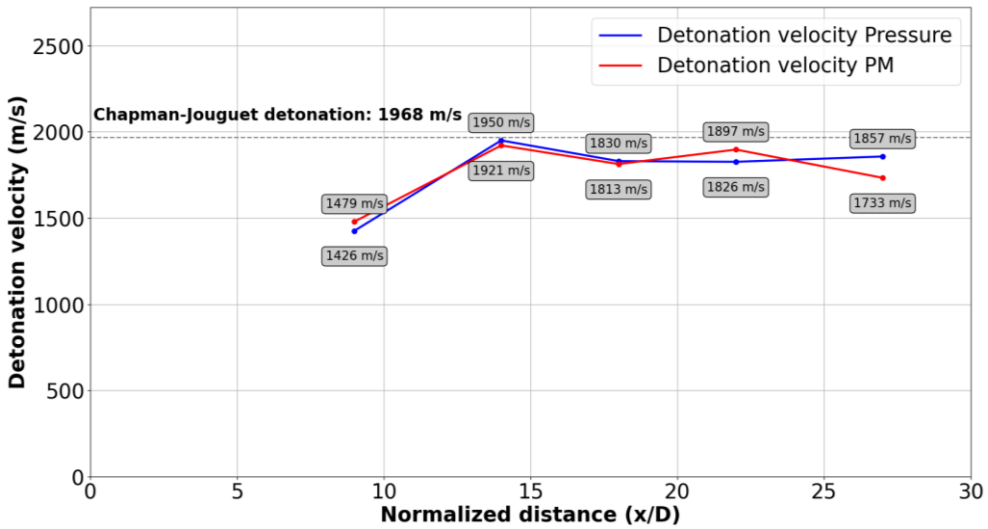

Figure 5: Comparison of the calculated velocity for the PM and pressure sensors for Plate 3

Once the detonation arrives at the end of the tube, a reflected shock wave is created. Likewise the incoming detonation, the time of arrival for the reflected shock wave can be estimated from the pressure sensors inside the extension. From the time of arrival of the reflected shock wave and the reference pressure, the impulse of the reflected shock can be calculated.

4.3 Impulse calculation and comparison

Once the state of the flame approaching the reflection end is known and corresponding to a detonation state, the impulse from the pressure sensors inside the extension can be calculated and compared. Then the impulse at the non-deformable flange can be compute from the Flange experiments. If the impulses of the incoming detonation are similar between Plate and Flange experiments, the pressure signal at the non-deformable flange could be considered as the load applied to the plate in a Plate experiment. The impulses calculation for the incoming shock will be limited by the arrival of the reflected shock. Thus the impulses will be calculated and displayed up to 0.2 ms after the time of arrival for both incoming detonation and reflected shock.

First, the impulses of the incoming detonation are compared for pressure sensor P1 for all the experiments. The incoming impulse for all the experiment are displayed in Fig. 6, at t = 0.2 ms the maximum difference in impulse is 0.00014 bar.s or 6% taking the maximum value as reference. A great repeatability of the impulse behavior is shown for the incoming detonation and the differences between the impulses are negligible and might be due to the difference in Hydrogen concentration in the initial mixture.

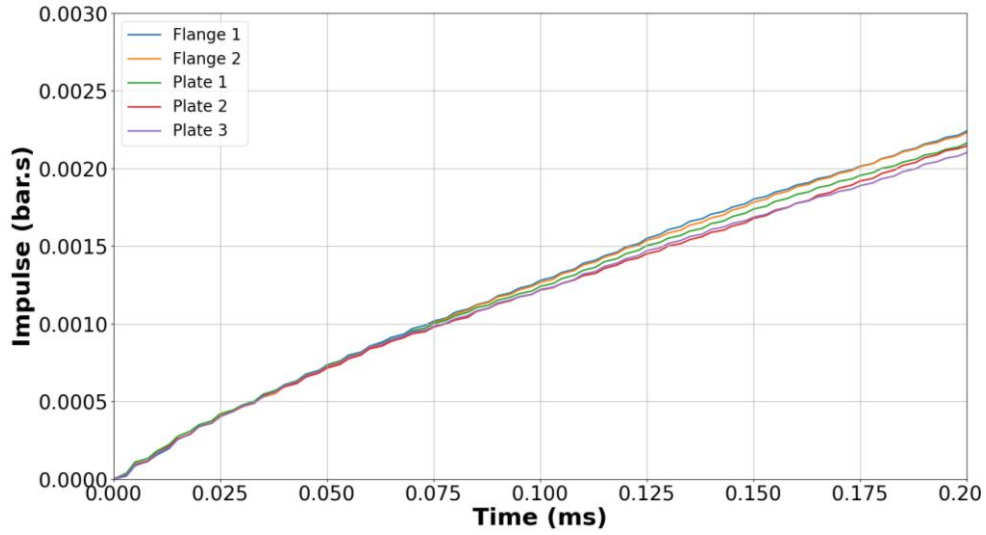

Figure 6: Impulse of the incoming detonation for and P1 pressure sensor

Now that the incoming detonation for all the experiments has been observed to be similar, the first step to investigate the FSI effects is to compare the impulse from the incoming and reflected shock. In Fig. 7, the reflected impulse can be observed for the same experiments as previously.

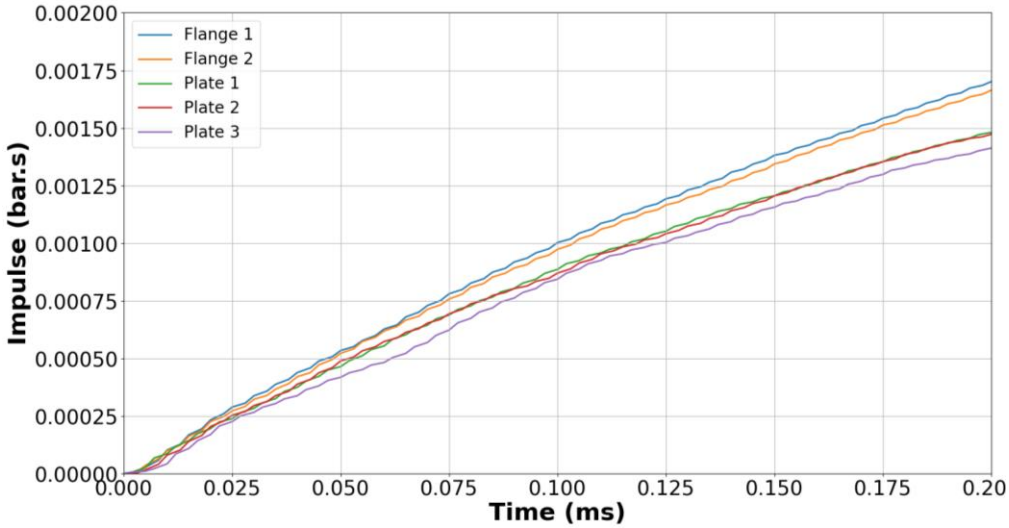

Figure 7: Impulse of the reflected shock P1 pressure sensor

The reflection of the detonation reduce in a systematic way the impulse when comparing the incoming detonation and reflected shock. However, it can be observed that there is a non-negligible difference between the Flange and Plate experiments. In the following, the comparison of the impulse will be done for the pressure sensor P1. In order to compare more effectively the amount of impulse involved in the FSI effects, a relative impulse difference is introduced in Equation (6).

$$I_{rel} = \frac{|I_{R-Plate} - I_{R-Flange}|}{I_{R-Flange}}, \tag{6}$$

Where I_R stand for the reflected impulse. To avoid mathematical error during the calculation of this value, it is calculated from $t = 0.025\ ms$. This value has been calculated for each Plate experiment at the pressure sensor P1, taking Flange 1 as reference. This relative impulse is shown for every Plate experiment in Fig. 8.

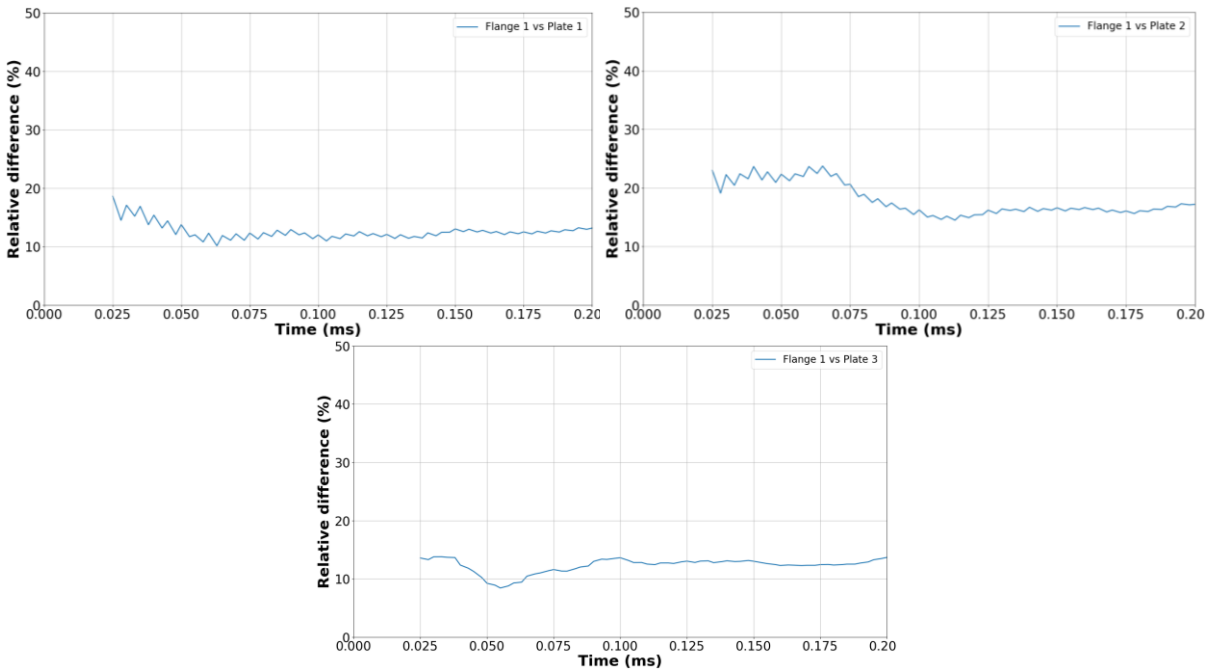

Figure 8: Relative impulse difference for Plate 1 (Up-Left) Plate 12(Up-Right) and Plate 3 (Down)

It can be observed that the relative impulse difference stabilize around a value of 15% for all experiments, regardless the thickness of the plate. From Equations (1) and (2), it can be observed that the deflection to thickness ratio is proportional to the inverse of the thickness squared. As the amount of impulse involved in the plate deformation is observed to be the same for every FSI experiments. The other parameters being geometrical or material constant, the only parameter of influence seems to be the thickness of the plate. Thus reducing the thickness by a factor 2 will raise the deflection to thickness ratio by a factor 4, which is what is observed looking at Table 6. Then, knowing the deflection to thickness ratio from the Plate experiments, it is possible to reversely use equation (1) and (2) to estimate the quantity of impulse involved in the plate deformation and compare this value to the impulse from the full flange sensor P11. The impulses derived from the Nurick correlation are in Table 6.

Table 6: Deformation data from plate experiments

Case	Central deflection (mm)	Thickness (mm)	Static yield stress (MPa)	Deflection to thickness ratio	Impulse from Nurick's correlation (bar.s)
Plate 1	9.4	1.01	210	9.3	0.0046
Plate 2	17.7	0.48	210	36.9	0.0042
Plate 3	16.8	0.48	210	35.2	0.0040

In our experiments, a laser has been employed to dynamically measure the deformation at the center of the plate. Even though these data have not been fully post-processed yet, a first estimation of the deformation duration is estimated around 0.2-0.3 ms for both plate thicknesses. From the impulses computed from the Nurick correlation in Table 6, it is possible to estimate the time needed to reach this impulse for a Flange experiment and compare it to the deformation time. From the Flange pressure sensor on Fig. 9 it can be observed that the estimated time to reach these impulses lies between 0.17-0.22 ms, which is not far away from the first estimation of deformation time. Further investigations are planned on this point.

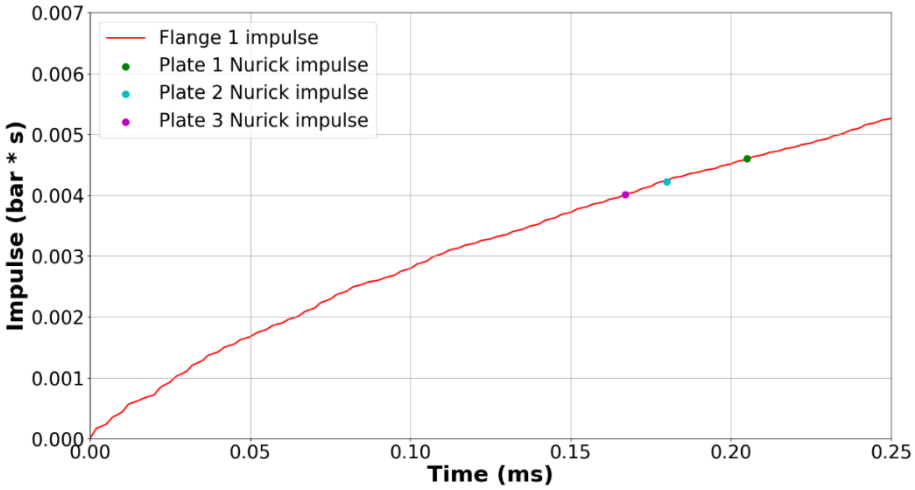

Figure 9: Impulse from Nurick correlation compared to Flange 1 pressure sensor

5.0 CONCLUSIONS AND OUTLOOK

This contribution was focused on the analysis of the detonation experiments performed on the SSEXHY facility. Several experiments has been conducted with different configuration, with and without deformable plates. The state of the detonation was compared before and after reflection for Flange and Plate experiments. An acceptable repeatability has been shown in the presented experiments, as all experiments reach detonation state consistently with velocities and pressure close to the expected theoretical values.

Looking at the impulse close to the reflection end in the presented experiment, a systematic decay in the impulse has been observed when comparing the reflected impulse from a Flange to a Plate experiment. The fluid-structure interaction effects are significant in the variation of the impulse compared to a simple reflection, in the order of 15% no matter the thickness of the plate. The same amount of impulse seems to be involved in the plate deformation and the behavior of the plate deformation correlate well with previous work on plate deformation under impulsive load. It seems that the first instant of the impulse are critical for the plate deformation. Comparing the deformation of thin plates under a gaseous detonation with the Nurick correlation derived from solid explosive shows a similar behavior.

Further experiments with other plate thicknesses should be undertaken for repeatability purpose. Furthermore other initial hydrogen concentration have been investigated, especially 15% in paper ID115. For this initial concentration, the impulse is observed to be greater in the first instants after the impact as it can be observed in Fig. 10.

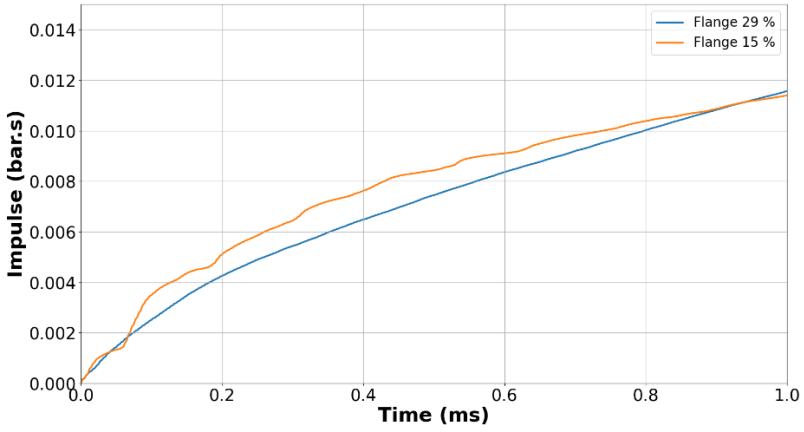

Figure 10: Impulse comparison for 15% and 29% at the center of the Flange

ACKNOWLEDGMENT

This work has been performed with a financial support of the French Atomic Energy and Alternative Energies Commission (CEA Paris-Saclay center) and the Electricité de France (EDF) in the framework of the Generation II & III reactor program.

REFERENCES

1. H.G., Ng and J.H.S. Lee, Comments on explosion problems for hydrogen safety, *Journal of loss and prevention*, **21**, 2007, pp. 136-146.
2. V. Aune et al., Fluid-structure interaction effects during the dynamic response of clamped thin steel plates exposed to blast loading, *International Journal of Mechanical Sciences*, **195**, 2021.
3. E. Studer et al., Detailed examitation of deformations induced by internal hydrogen explosions: part 1 experiments, 2017
4. E. Studer et al., Detailed examitation of deformations induced by internal hydrogen explosions: part 2 models, 2017
5. J.S. Damazo, Planar reflection of gaseous detonation, PhD Thesis, 2013
6. D.L. Chapman, On the rate of explosion in gases. *Philosophical magazine*, **47**, 1899, pp. 90-104.
7. E. Jouguet, On the propagation of chemical reaction in gases, *Journal de Mathematiques Pures et Appliquées*, **1**, 1905, pp. 347-425.
8. CEA NASA code, https://cearun.grc.nasa.gov, visited on 24/03/2023
9. G Nurick and J. Martin. Deformation of thin plates subjected to impulsive loading - A Review, Part I: Theoretical considerations. *International Journal of impact engineering*, **8,** 1989, pp. 159–170.
10. G.N. Nurick and J. Martin. Deformation of thin plates subjected to impulsive loading - A Review, Part II: Experimental studies. *International Journal of impact engineering*, **8**, 1989, pp171–186.
11. G.N. Nurick and S. Chung Kim Yuen. Deformation of thin plates subjected to impulsive loading - A Review, Part III: An update 25 years on. *International Journal of impact engineering*, **107**, 2017, pp. 108–117.
12. R. Scarpa, Mécanisme d'accélération d'une flame de prémélange hydrogène/air et effets sur les structures, PhD Thesis, 2017
13. I. Barsoum, Z.Barsoum and M.D. Islam. Thermomechanical Evaluation of the Performance and Integrity of a HDPE Stub-End Bolted Flange Connection. *Journal of Pressure Vessel Technology*, **141**, 2019.
14. T.A. Duffey, R.R. Karpp and T.R. Neal. Response of containment vessels to explosive blast loading. *Pressure Vessel and Piping Division Conference (ASME)*, 1982.
15. M. Kusnetsov et al., Effect of Obstacle Geometry on behavior of turbulent flames. Forschungszentrum Karlsruhe, *Technik und Umwelt*, 1999.